Mechanical Testing of Shale by Instrumented Indentation

Application Note

Jennifer Hay,
Agilent Technologies

Carl H. Sondergeld,
Mewbourne School of Petroleum and Geological Engineering,
Mewbourne College of Earth and Energy, University of Oklahoma
Norman, OK

Introduction

Shale is a fine-grained rock often composed of clay and other minerals. The predominance of clays influences its mechanical properties and typically imparts a strong elastic anisotropy. Shales are often rich in organic material called kerogen which acts as a source during hydrocarbon generation. Shale formations are interesting to the oil and gas industry because they host vast natural gas and oil resources. Gas flows to the wellbore primarily through natural and induced fractures. The natural fractures are caused by tectonic forces, desiccation and hydrocarbon generation while the process of hydraulic fracturing stimulates and induces fractures.

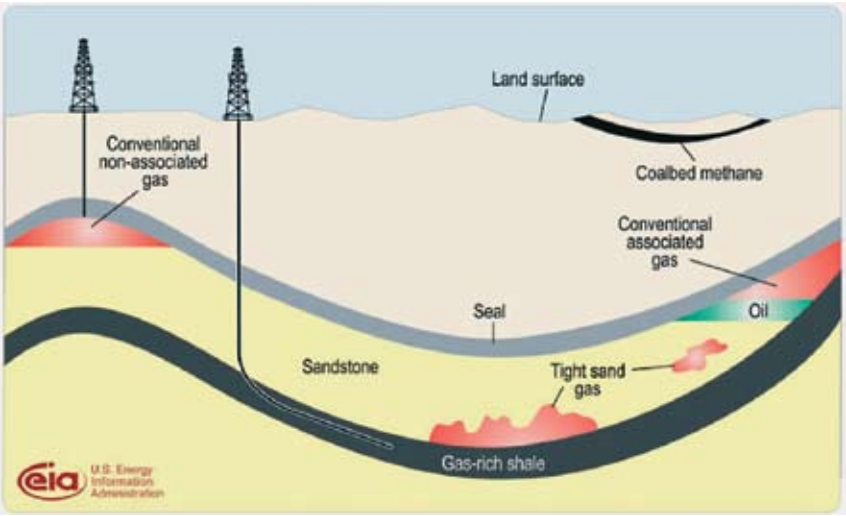

Figure 1. Schematic geology of natural gas resources. (U. S. Energy Information Administration).

Advances in drilling technology—specifically the ability to drill laterally and induce multiple massive hydraulic fractures—have increased profitability of shale gas. Thus, the ability to form extensive, stable fractures in the shale is directly related to the profitability of gas production from shales [1].

Mechanical properties are necessary in the design of these fractures; however, because of the mineralogical variability of shale, mechanical properties vary considerably. Many shales are chemically and mechanically unstable making recovery of suitably sized samples for standard mechanical testing impossible. Nano-indentation testing of drill cuttings, fragments or sidewall cores provides a viable and economically attractive option for recovering needed mechanical properties. Thus, the purpose of this work was to use instrumented indentation testing to measure the mechanical properties of small volumes of shale. Details of instrumentation and analysis are explained elsewhere [2-4]. Instrumented indentation yields a force-displacement *(P-h)* trace, Young's modulus *(E)*, and hardness *(H)*.

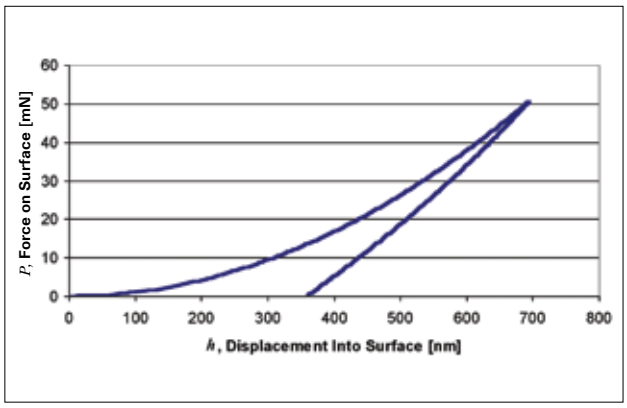

Figure 2. Typical force-displacement curve for an instrumented indentation test. Permanent work, W_p, is the area between the curves.

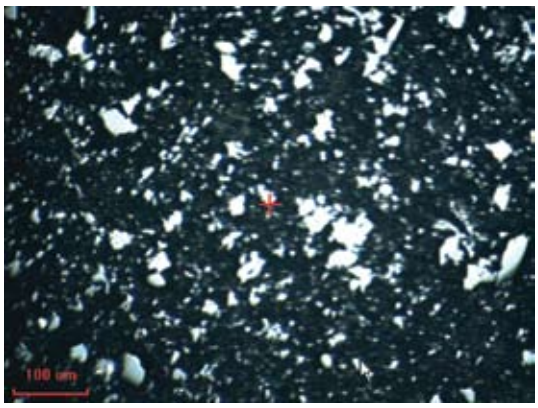

Figure 3. Barnett shale surface, as prepared for indentation.

Observed correlations have led researchers to conclude that shale is most likely to fracture easily and well if it has a high Young's modulus and low Poisson's ratio (ν) [1, 5]. An alternative parameterization based on mineralogy suggests brittleness or "fracability" is dependent on quartz content. A more conclusive parameterization is desirable. Both Young's modulus and Poisson's ratio are elastic properties which are imprecisely related to "fracablity." For a given stress, they predict the resulting strain (or vice versa) *only up to the point of permanent deformation.* Although they tell how stresses grow elastically they contain no information about the threshold criteria for permanent deformation marked by the onset of fracture, plastic yield, or other mechanism.

So there is room for improvement in predicting fracture in shale. Instrumented indentation has been used to measure fracture toughness in glasses and ceramics by measuring the average length, c, of cracks emanating from the corners of residual impressions [6]. The average crack-length, c, is related to fracture toughness, K_c, through the expression

$$K_c = \alpha \left(\frac{E}{H}\right)^{1/2} \left(\frac{P_{\max}}{c^{3/2}}\right) \quad , \quad \text{Eq. 1}$$

where α is an empirical constant that depends on the geometry of the indenter. Unfortunately, shale is too heterogeneous at the microscopic scale for this technique to be feasible. However, solving Eq. 1 for crack length, c, gives us significant insight:

$$c = \alpha * \left(\frac{E}{H}\right)^{1/3} \left(\frac{P_{\max}}{K_c}\right)^{2/3} \quad . \quad \text{Eq. 2}$$

Eq. 2 indicates that for a given fracture toughness and applied force, *the length of the resulting crack depends on the ratio of Young's modulus to hardness.* Eq. 2 supports the observed correlation that longer cracks are sustained in shale of high Young's modulus. The inverse relationship to hardness is sensible, because hardness is a measure of the material's resistance to permanent damage. Thus, though others have suggested that a high value of $E/\nu$is advantageous, we suggest that the dimensionless parameter E/H contains more information about the ability to generate and sustain cracks.

But perhaps we have an even simpler and more relevant parameter at our disposal. The most basic output of an instrumented indentation test is a force-displacement curve, illustrated schematically in Figure 2. The origin of this plot is the point at which the indenter first contacts the test surface. As the applied force increases, the displacement increases as well, until the peak test force is achieved. Then, as the contact force decreases, some of the displacement is generally recovered, though usually not all. If the contact were completely plastic, then the unloading curve would be exactly vertical. If the contact were completely elastic, then the unloading curve would coincide with the loading curve.

The areas defined by the force-displacement curve have the units of work: force times distance. Specifically, we define three areas. The permanent work *(W_p)* is the area within the force-displacement curve, bounded below by the axis $P = 0$. The elastic work *(W_e)* is the recovered area, or the area bounded by the unloading curve, the line $h = h_{max}$, and the axis $P = 0$. The total work is equal to the sum of the elastic work and permanent work: $W_t = W_e + W_p$. To reduce the dependence on indent size, we consider W_e and W_p with respect to W_t. That is, we define the normalized parameters W^*_e and W^*_p as

$$W^*_e = W_e / W_t, \text{ and}$$

$$W^*_p = 1 - W^*_e$$

We suggest that W^*_p is a valuable parameter for this application, because it quantifies the fraction of indentation work which goes into causing permanent damage. If W^*_p is zero, then all of the work is recovered – the indentation does not cause any permanent damage. If W^*_p is 100%, then all of the work of indentation is accommodated by permanent damage. Presumably, the dominant mechanisms for this damage are microfracturing and plastic yielding.

Experimental Method

A sample of Barnett shale was tested in this work. Barnett shale formation covers about 5000 mi^2 in Texas with the richest reserves located in Dallas-Fort Worth area. This formation may contain the largest reserve of natural gas in the United States [7]. The plug was metallographically mounted and polished. The final polish was with 0.5 µm diamond grit. Figure 4 shows an optical image of the prepared surface.

An Agilent G200 NanoIndenter having the high-load option was used for this work. The high-load option allowed us to make indents that were large relative to microstructural features. This was important since the goal was to use instrumented indentation to measure bulk properties. With this option, the G200 can apply forces up to 10N. All tests were performed according to ISO 14577, which is an international standard for instrumented indentation testing [8].

Four sets of tests were performed:

- 100 large tests in the shale,
- 15 small tests, all contained within the single particle shown in Figure 5,
- 12 large tests in the fused-silica reference block, and
- 10 small tests in the fused silica reference block.

After indentation testing was complete, energy-dispersive X-ray spectroscopy (EDX) was utilized to determine the material composition at specific test sites.

Results and Discussion

Results for all tests are summarized in Table 1. The average Young's modulus for the shale is 26.9 + 2.1 GPa. Previous measurements on gas shales including the Barnett shale indicate the Young's modulus varies from as low as 7 GPa to as high as 77 GPa [9] with an average of 26.6 GPa, which is remarkably similar to the indention value.

The SEM images of Figure 4 confirm that indents are large enough to sample all relevant elements of this shale, including clay and mineral grains. The mode and degree of fracturing vary from site to site. In Figure 4a, cracks are concentrated within the mineral grains and around their boundaries, whereas the clay seems to inhibit crack growth. In Figure 4b, the areas of concentrated mineral grains show extensive fracture. Figure 4c shows a chip as well as fracture around the boundary of the impression. These images corroborate and help explain the proposition that brittleness is related to quartz content.

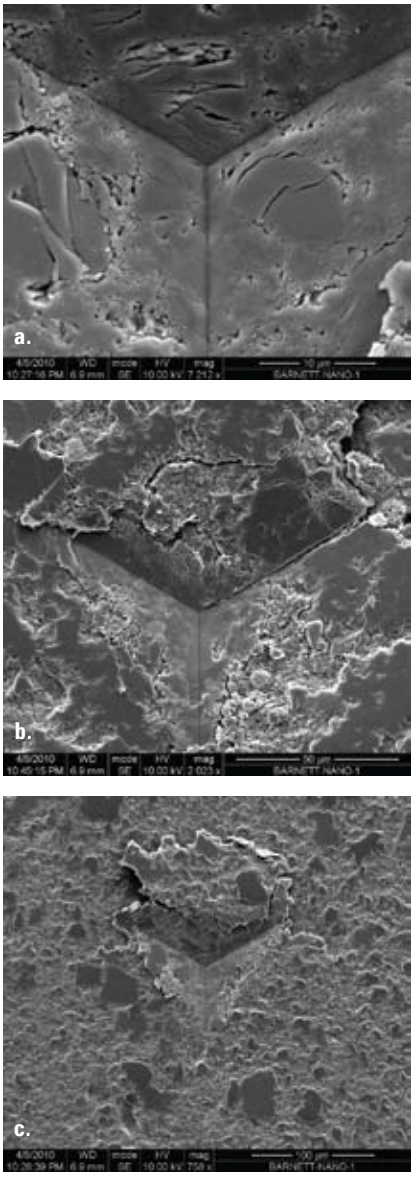

Figure 4. SEM images of three residual impressions in shale showing (a) fracture within and around mineral grains, (b) pervasive fracture, especially in areas of concentrated mineral grains, and (c) fracture around the perimeter of the indent and chipping.

Material	Peak Force	N Tests	N Valid Tests	Displacement†	Modulus	Hardness	W*p
	N			nm	GPa	GPa	%
Shale	5.0	100	98	17200±1390	26.9±2.1	0.91±0.16	72.5±3.3
Dolomite Particle	0.01	15	13	316±9	95.4±2.7	5.80±0.43	61.1±1.4
Silica	5.0	12	12	6840±66	73.4±1.7	9.08±0.16	34.8±1.5
Silica	0.01	10	10	297±1	73.0±0.4	9.00±0.08	36.0±0.1

Table 1. Summary of Indentation Measurements

† The diameter of the indentation is about 7X this value.

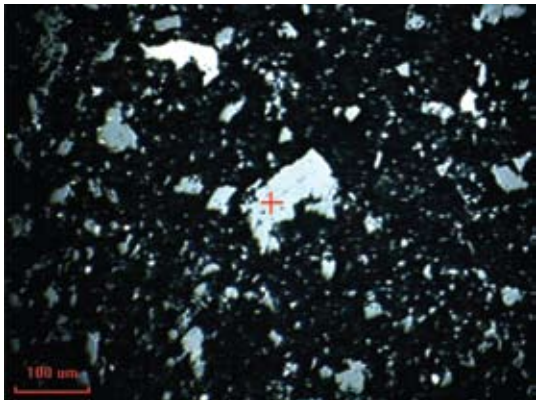

Figure 5. Fifteen sub-micron tests were placed in the relatively large dolomite grain in the center of this image.

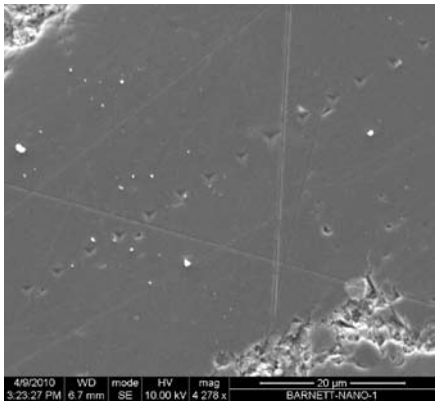

Figure 6. Indents in the dolomite imaged in Figure 5.

Post-indentation EDX indicates that the particle at the center of Figure 5 is dolomite—calcium magnesium carbonate $CaMg(CO_3)_2$. Dolomite has a range of reported modulus from 76 to 93 GPa [10]. By indentation, we measured the Young's modulus of this particle to be 95.4+2.2 GPa. The SEM image in Figure 6 shows the residual impressions in this mineral. They are quite small, because the prescribed test force was only 10 mN, and because the material is both hard and elastic.

Results for the fused silica reference material are consistent with known properties; these results verify that the testing instrument is functioning properly.

Figure 7 shows a force-displacement curve for a single large indent (to 5 N) in the shale. The dark area is the work that went into permanently deforming the material, presumably by micro-scale fracture. Dividing the dark area by the total area (the sum of the light and dark areas) gives the normalized permanent work, W^*_p. We hypothesize that this parameter is a good predictor of the propensity to generate extensive cracking in shale formations. Further testing will be needed to validate or invalidate this hypothesis. At least for this material, W^*_p is linearly related to the ratio of Young's modulus to hardness as shown in Figure 8.

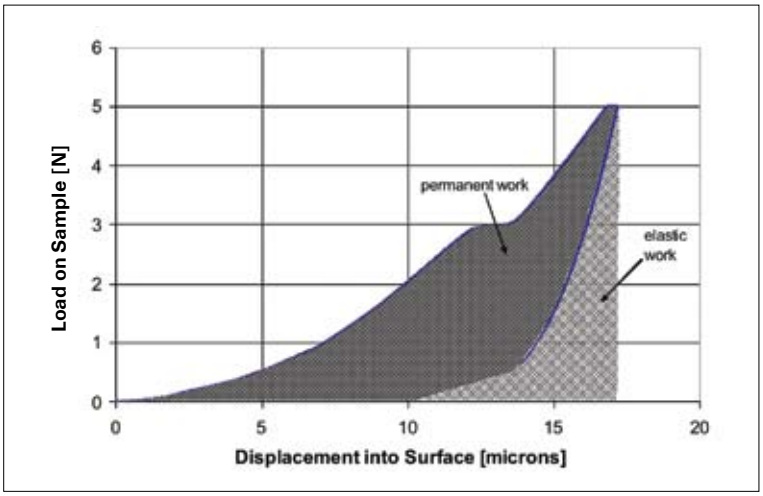

Figure 7. Force-displacement curve from a single large test in the shale. Fracture causes the "step" at a force of 3N. The dark area is the work which causes permanent deformation.

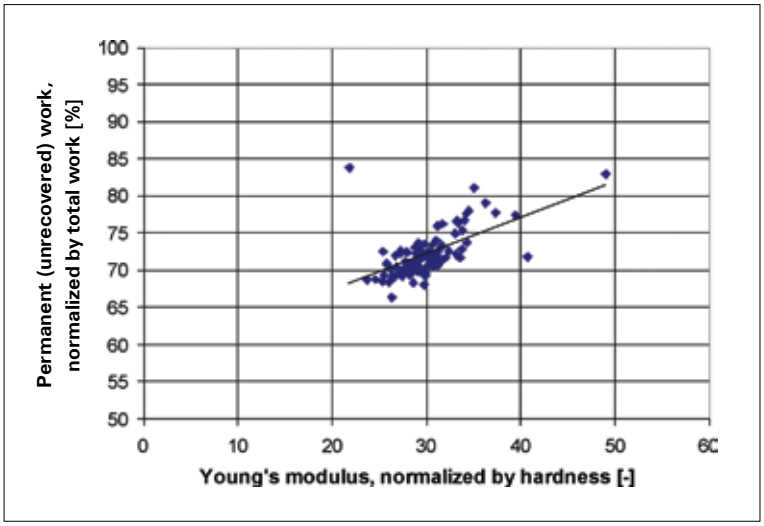

Figure 8. Linear trend relates W^*_p to E/H.

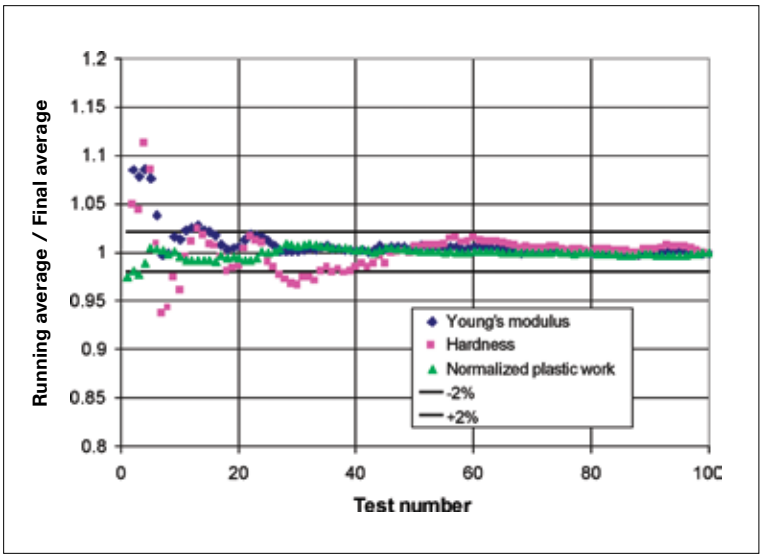

Figure 9. Convergence of results to their final values. Normalized permanent work is within 2% of its final value after only 3 tests. Convergence of Young's modulus and hardness takes longer (25-40 tests) due to their dependence on the evaluation of contact area.

Because shale is so heterogeneous, we wanted to know how many indentation tests would be needed in order to get reliable averages. This was the reason for doing a very large number of indents on the shale. The total time to complete all 100 tests on the shale was 10 hours; testing was completely unattended.

Figure 9 shows how the averages converged to their final values. To generate this plot, we computed the running average after first test, second test, third test, etc., and divided by the average computed after the hundredth test. This plot provides another reason to prefer the parameter W^*_p to either Young's modulus or hardness independently or their ratio. W^*_p is within 2% of its final value after only 3 tests, while Young's modulus requires about 25 tests, and hardness requires about 40 tests.

The reason for the slow convergence of E and H relative to W^*_p is in how the values are calculated from the fundamental force-displacement data. The calculations of both E and H require the area of contact, A, between the indenter and the sample. The benefit of instrumented indentation is that this area is computed from the force-displacement data, not by imaging the residual impression [2]. However, this computation assumes that the test surface is smooth and uniform. Roughness and heterogeneity at the surface cause a higher degree of scatter in the determination of contact area. Furthermore, the calculation of hardness depends directly on A, while the calculation of Young's modulus depends on $A^{1/2}$. Therefore, scatter in the determination of contact area manifests twice as strongly in hardness as Young's modulus. This is why the convergence in hardness is the slowest. By contrast, the parameter W^*_p is calculated directly from the force-displacement data. Thus, W^*_p converges quickly to its final value.

Conclusions

An Agilent G200 NanoIndenter with high-load option was used to mechanically test Barnett shale according to a standard test method. The measured Young's modulus was 26.9+2.1 GPa, and the hardness was 0.907+0.159 GPa. Because of the heterogeneity of shale, forty tests were necessary to achieve reliable average values of Young's modulus and hardness. The instrument was also used to test a single dolomite particle within the shale, giving a Young's modulus of 95.4+2.7 GPa and a hardness of 5.80+0.43 GPa. Thus, we have demonstrated the utility of nanoindentation for measuring the mechanical properties of the bulk shale as well as individual constituents of the same.

The measurement of a promising dimensionless parameter was also demonstrated: the normalized permanent work, or W^*_p. We hypothesize that this parameter will be a good predictor of the propensity for extensive fracture in shale formations. Further testing is needed to validate or invalidate this hypothesis.

References

1. R.M. Bustin, A. Bustin, D. Ross, G. Chalmers, V. Murthy, C. Laxmi, and X. Cui, "Shale Gas Opportunities and Challenges," Search and Discovery Articles, No. 40382, 2009. http://www.searchanddiscovery.com/documents/2009/40382bustin/ndx_bustin.pdf
2. W.C. Oliver and G.M. Pharr, "An Improved Technique for Determining Hardness and Elastic Modulus Using Load and Displacement Sensing Indentation Experiments," *J. Mater. Res.,* Vol. 7 (No. 6), 1992, p 1564–1583.
3. J.L. Hay, "Introduction to instrumented indentation testing," *Experimental Techniques,* Vol. 33, No. 6, pp. 66–72, 2009.
4. P.A. Agee, "Instrumented Indentation Testing with the Agilent Nano Indenter G200," Agilent Application note: http://cp.literature.agilent.com/litweb/pdf/5990-4905EN.pdf
5. B. Grieser and J.Bray, "Identification of Production in Unconventional Reservoirs," SPE 106623 SPE Production and Operations Symposium, Oklahoma City, OK, 31 March–3 April, 2007
6. D. Harding, W.C. Oliver, G.M. Pharr, "Cracking during nanoindentation," *MRS Symp. Proc.,* Vol. 356, pp. 663–668, 1995.
7. "Bounty from Below: The impact of developing Natural Gas Resources associated with the Barnett shale on business activity in the Fort Worth and the Surrounding 14-county area," A presentation by The Perryman Group, May 2007. http://www.barnettshaleexpo.com/docs/Barnett_Shale_Impact_Study.pdf
8. "Metallic materials — Instrumented indentation test for hardness and materials parameters," ISO 14577, 2002.
9. C.H. Sondergeld, K.E. Newsham, J. Comisky, M.R. Rice , C.S. Rai, "Petrophysical Considerations in Evaluating and Producing Shale Gas Resources," SPE 131768, extended abstract, SPE Unconventional Gas Conference, Pittsburgh, Pennsylvania, USA, 23–25 February 2010.
10. F. Birch, "Compressibility; Elastic Constants," in Handbook of Physical Constants, ed by. S.P. Clark, The geological Society of America, Memoir 97, 97-173, The Geological Society of America, New York, 1966.

AFM Instrumentation from Agilent Technologies

Agilent Technologies offers high-precision, modular AFM solutions for research, industry, and education. Exceptional worldwide support is provided by experienced application scientists and technical service personnel. Agilent's leading-edge R&D laboratories are dedicated to the timely introduction and optimization of innovative and easy-to-use AFM technologies.

www.agilent.com/find/afm

Americas

Canada	(877) 894 4414
Latin America	305 269 7500
United States	(800) 829 4444

Asia Pacific

Australia	1 800 629 485
China	800 810 0189
Hong Kong	800 938 693
India	1 800 112 929
Japan	0120 (421) 345
Korea	080 769 0800
Malaysia	1 800 888 848
Singapore	1 800 375 8100
Taiwan	0800 047 866
Thailand	1 800 226 008

Europe & Middle East

Austria	43 (0) 1 360 277 1571
Belgium	32 (0) 2 404 93 40
Denmark	45 70 13 15 15
Finland	358 (0) 10 855 2100
France	0825 010 700* *0.125 €/minute
Germany	49 (0) 7031 464 6333
Ireland	1890 924 204
Israel	972-3-9288-504/544
Italy	39 02 92 60 8484
Netherlands	31 (0) 20 547 2111
Spain	34 (91) 631 3300
Sweden	0200-88 22 55
Switzerland	0800 80 53 53
United Kingdom	44 (0) 118 9276201

Other European Countries:
www.agilent.com/find/contactus

Printed in USA, May 5, 2010
5990-5816EN

Agilent Technologies